



Contents lists available at [ScienceDirect](http://ScienceDirect)

## The International Journal of Biochemistry & Cell Biology

journal homepage: [www.elsevier.com/locate/biocel](http://www.elsevier.com/locate/biocel)



# Endothelial CD146 is required for *in vitro* tumor-induced angiogenesis: The role of a disulfide bond in signaling and dimerization

Chaogu Zheng<sup>a,b,c</sup>, Yijun Qiu<sup>a,b</sup>, Qiqun Zeng<sup>a,b,c</sup>, Ying Zhang<sup>a,b,c</sup>, Di Lu<sup>a,b</sup>, Dongling Yang<sup>a,b</sup>, Jing Feng<sup>a,b</sup>, Xiyun Yan<sup>a,b,\*</sup>

<sup>a</sup> National Laboratory of Biomacromolecules, Institute of Biophysics, Chinese Academy of Sciences, Beijing 100101, China

<sup>b</sup> Chinese Academy of Sciences–University of Tokyo Joint Laboratory of Structural Virology and Immunology, Institute of Biophysics, Chinese Academy of Sciences, Beijing 100101, China

<sup>c</sup> Graduate University of Chinese Academy of Sciences, Beijing 100049, China

### ARTICLE INFO

#### Article history:

Received 26 December 2008  
Received in revised form 14 March 2009  
Accepted 29 March 2009  
Available online xxx

#### Keywords:

CD146  
NFκB  
Disulfide bond  
Dimerization  
Tumor angiogenesis

### ABSTRACT

Tumor angiogenesis, induced by tumor-secreted pro-angiogenic factors, is an essential process for cancer development and metastasis. CD146 is identified as an endothelial cell adhesion molecule and implicated in blood vessel formation, however, its exact role in angiogenesis, particularly tumor angiogenesis, and its potential function of mediating downstream signaling are still unclear. In present study, we evidenced that silencing endogenous endothelial CD146 by RNAi significantly impaired hepatocarcinoma cell secretions-promoted tubular morphogenesis and -enhanced motility of endothelial cells. Biochemical studies revealed that CD146 was required for the activation of p38/IKK/NFκB signaling cascade and up-regulation of NFκB downstream pro-angiogenic genes, notably IL-8, ICAM-1 and MMP9, in response to tumor secretions. Interestingly, specific anti-CD146 mAb AA98, which bound a conformational epitope depending on C452–C499 disulfide bond, could abrogate NFκB activation and tumor angiogenesis, whereas another anti-CD146 mAb AA1 recognizing a linear epitope containing aa50–54 did not have such effects. Further structure–function analysis identified that C452–C499 disulfide bond within the fifth extracellular Ig domain was indispensable for CD146-mediated signaling and tube formation. Moreover, dimerization of CD146, which was enhanced by tumor secretions and suppressed by AA98 but not AA1, also relied on C452 and C499. Together, this study for the first time uncovered the pro-angiogenic role of CD146 and also pinpointed the key structural basis responsible for its signaling function and dimerization. These findings also suggested that CD146 might serve as not just a cell adhesion molecule but also a membrane signal receptor in tumor-induced angiogenesis.

© 2009 Elsevier Ltd. All rights reserved.

## 1. Introduction

Tumor angiogenesis, the proliferation of a network of blood vessels in tumor microenvironment that penetrates into cancerous growth, provides oxygen and nutrients and removes wastes for hyperproliferated cancer cells. Thus, it is an early and crucial step for the development and metastasis of solid tumor. Previous studies evidenced that most cancer cells secrete a variety of pro-angiogenic cytokines and chemokines, such as fibroblast growth factors, vascular endothelial growth factors, IL-1, IL-6, IL-8 and stromal cell-derived factor 1, which induce the survival, proliferation and migration of endothelial cells and eventually promote tumor angiogenesis.

Pro-inflammatory cytokines, such as TNF-α and IL-1β, produced by cancer cells and infiltrated immune cells in tumor, were found to activate NFκB in endothelial cells (Bowie et al., 1996) and promote angiogenesis (Leibovich et al., 1987; Voronov et al., 2003). Activated NFκB, composed of two principal subunits, p65 and p50, were released from the association with inhibitory subunit IκB and translocated into nucleus to modulate the expression of downstream genes (Barnes and Karin, 1997). NFκB activates the transcription of pro-angiogenic factors, such as IL-8, IL-6, MCP-1 and VEGF, and endothelial cell adhesion molecules, such as ICAM-1, VCAM-1 and E-selectin as well as matrix metalloproteinases, MMPs, which play as important effectors in endothelium activation (Blackwell and Christman, 1997; Monaco and Paleolog, 2004; Roebuck, 1999; St-Pierre et al., 2004). In the other hand, Miyake et al. (2006) reported that NFκB decoy oligodeoxynucleotides significantly inhibited neointimal hyperplasia in rabbit vein graft model, supporting the promotive role of NFκB in blood vessel formation. In addition, studies evidenced that oxidative stress and hypoxia, often observed in tumor microenvironment, also induced

\* Corresponding author at: No. 15 Datun Road, Chaoyang District, Beijing 100101, China. Tel.: +86 10 6488 8583; fax: +86 10 6488 8584.

E-mail address: [yanxy@sun5.ibp.ac.cn](mailto:yanxy@sun5.ibp.ac.cn) (X. Yan).

the activation of endothelial NF $\kappa$ B and expressions of chemokines and antioxidant proteins, including NOS, COX-2 and MnSOD, which enhanced local endothelial stability and mortality (Shono et al., 1996; Murley et al., 2001; Naidu et al., 2003; Zhen et al., 2008). Therefore, NF $\kappa$ B plays a critical role in activating endothelial cells during tumor angiogenesis.

CD146 was originally cloned from human melanoma cells as a melanoma specific cell adhesion molecule (Johnson et al., 1993) and then identified to be expressed on circulating endothelial cells (Bardin et al., 1996). The extracellular region of CD146 contains a characteristic V-V-C2-C2-C2 immunoglobulin-like domain structure. Within each domain a pair of cysteines theoretically forms a disulfide bond to support the protein structure. The acts of CD146 as an adhesion molecule in enhancing cell adhesion and migration were studied in both melanoma and endothelial cells (Xie et al., 1997; Guezzuez et al., 2007; Kang et al., 2006), whereas its role in mediating signal transduction is not clear. Although Anfosso et al.'s studies found that CD146 cross-linking by a monoclonal antibody (mAb), named S-endo1, triggered the phosphorylation of FAK through association with Fyn (Anfosso et al., 1998, 2001), these artificial engagements of CD146 might not reflect its physiological function. Moreover, the signaling of Fyn/FAK/paxilin they established mainly mediated cytoskeleton rearrangement and cell adhesion, indicating additional pathway might exist for some other functions of CD146, such as mediating angiogenesis.

Our previous studies showed that a novel therapeutic anti-CD146 mAb, namely AA98, significantly inhibited tumor angiogenesis possibly through inhibiting endothelial NF $\kappa$ B activation (Yan et al., 2003; Bu et al., 2006). However, the exact role of CD146 in angiogenesis is unknown and the direct evidence linking CD146 to the activation of NF $\kappa$ B signaling is still missing. Furthermore, we previously observed the dimerization of CD146 in living cells using FRET method and found that its dimerization was inducible and regulatable under certain circumstances (Bu et al., 2007). Nevertheless, the potential role of dimerization in mediating signal transduction is unclear; also, the structural basis of CD146 dimerization has never been investigated.

In this study, we aimed to clarify the function of CD146 in tumor-induced angiogenesis and elucidate its downstream signaling by stimulating human endothelial cells with tumor secretions and silencing the endogenous CD146 expression by specific siRNA.

## 2. Materials and methods

### 2.1. Antibodies and reagents

All reagents and chemicals were purchased from Sigma (St. Louis, MO), and cell culture mediums were from Gibco (Grand Island, NY). The following antibodies were used in this study: anti-human NF $\kappa$ B p65, NF $\kappa$ B p50 (Upstate, Millipore Corporation, Billerica, MA), I $\kappa$ B $\alpha$ , phosphor-p38 MAPK $\alpha$ , Histone H1, Actin (Santa Cruz Biotech, Santa Cruz, CA), p38 MAPK $\alpha$ , IKK $\alpha$ , IKK $\beta$ , phosphor-IKK $\alpha$ (Ser<sup>180</sup>)/IKK $\beta$ (Ser<sup>181</sup>), phosphor-I $\kappa$ B $\alpha$  (p-Ser<sup>32/36</sup>) (Cell Signaling, Danvers, MA). Anti-His-tag, Myc-tag and FLAG-tag antibodies, as well as, Horseradish peroxidase (HRP) or fluorescent reagent conjugated affinity purified secondary antibodies were purchased from Sigma. Mouse anti-human CD146 mAbs, AA98 and AA1, were purified from ascites by protein A-Sepharose. Anti-IL-1 $\beta$  neutralizing antibody was purchased from BD Bioscience (San Jose, CA) and p38 inhibitor SB203580 and PI3K inhibitor LY294002 was purchased from Sigma.

### 2.2. Cell culture and transfection

Human melanoma cell A375, hepatocarcinoma SMMC 7721 cell line and Chinese Hamster Ovary (CHO) cells were obtained

from American Type Culture Collection (Rockville, MD). Primary human umbilical vein endothelial cells (HUVEC) were prepared from human umbilical cords as previously described (Jaffe et al., 1973). CHO cells were cultured in F12 medium containing 10% FCS and other cells were cultured in DMEM containing 10% FCS. Eugene HD (Roche) mediated transfection was employed according to the manufacture's instruction.

### 2.3. Plasmid constructs and dsRNA

On the basis of CD146 cDNA provided by Dr. Judith P. Johnson at University of Munich, DNA fragments encoding respectively CD146 fractions of D1–2, F44–227, F64–227, F84–227, F99–227 and F114–227 were cloned into pET30a expression vector. DNA fragments encoding respectively fractions of D2–3, D3–4 and D4–5 were cloned into pET32a. By site-directed mutagenesis, full-length mutants of CD146 cDNA with respective mutation at cysteines were generated in vector pcDNA3.1 on the basis of pcDNA3.1-CD146/wt; and then designated as CD146/C320A, CD146/C365A, CD146/C407A, CD146/C452A and CD146/C499A. In addition, three full-length CD146 mutants with targeted deletion at the region of aa50–59, aa50–54 and aa55–59 respectively were made by standard overlapping PCR, cloned into also pcDNA3.1 and designated as CD146/ $\Delta$ 50–59, CD146/ $\Delta$ 50–54 and CD146/ $\Delta$ 55–59.

Double-strand RNA (dsRNA) targeting respectively the CDS: 410–428 of CD146 and the CDS: 1562–1580 of GFP were synthesized by Invitrogen using the following sequences, siRNA-CD146: forward 5'-CCA GCU CCG CGU CUA CAA AdTdT-3', reverse 5'-UUU GUA GAC GCG GAG CUG GdTdT-3'; siRNA-GFP: forward 5'-CUU CAG CCU CAG CUU GCC GdTdT-3', Reverse 5'-CGG CAA GCU GAC CCU GAA GdTdT-3'.

### 2.4. Tube formation

Tube formation assay was performed as described by Nagata et al. (2003). Briefly, 24-well culture plates (Costar, Corning Incorporated) were coated with 200  $\mu$ l/well of Matrigel (BD Biosciences) followed by solidification for 30 min at 37°C. Cells transiently transfected with appropriate dsRNAs or plasmids were suspended at  $5 \times 10^5$  ml<sup>-1</sup> in complete RPMI 1640 medium or SMMC 7721-conditional medium. Then 200  $\mu$ l of this cell suspension was added into each well and were incubated for 6 h. Appropriate antibodies or normal IgG (50  $\mu$ g/ml) were directly added in the cell suspension when seeding. Tube formation was observed under an inverted microscope. Images were captured with a CCD color camera (Model, KP-D20AU, Hitachi, Japan) attached to the microscope and tube length was measured using the NIH Image J.

### 2.5. Cell migration assay

Cell migration was assayed using transwells (8  $\mu$ m pore size; Corning Costar) coated with type I collagen solution at 100  $\mu$ g/ml and blocked with 1% BSA in PBS. Cells under appropriate transfection were suspended in normal complete medium or SMMC 7721-conditional medium and then added to the upper chamber (5000 cells/well). Lower chambers contained fresh medium with 20%FBS, 10ng/ml human VEGF and bFGF. After incubation for 6 h, cells remained at the upper surface of the membrane were removed using a swab, while the cells that migrated to the lower membrane surface were fixed with ethanol and stained with Giemsa solution. The number of cells migrating through the filter was counted and plotted as the number of cells per optic field (20 $\times$ ). Either mAb AA98 or AA1 or mIgG (25  $\mu$ g/ml) was added to the upper chambers when cells were seeded.

## 2.6. Western blot

Whole cell extract were prepared by lysing cells in the NP-40 lysis buffer containing 50 mM Tris–Cl pH 6.8, 150 mM NaCl, 1 mM EGTA, 1%NP-40 and proteinase inhibitor cocktails (Roche). For preparing the nuclear extract, cytoplasmic membrane were disrupted in [0.5% NP-40, 25 mM Hepes (pH 7.5), 5 mM KCl, 0.5 mM MgCl<sub>2</sub>, 1 mM DTT and proteinase inhibitors]; then nuclei were collected by centrifuging and lysed in [25 mM Hepes (pH 7.5), 10% sucrose, 0.01%NP-40, 350 mM NaCl, 1 mM DTT and proteinase inhibitors]. Extracts were subjected to electrophoresis and transferred to nitrocellulose membranes (Millipore, Billerica, MA). The membranes were blocked with 5% nonfat dry milk in TBS with 0.1% Tween-20 for 2 h before the appropriate antibody was added and continued incubating for another 45 min. HRP conjugated secondary antibodies and enhanced chemiluminescence detection (Pierce, Rockford, IL) was used to detect the specific immunoreactive proteins.

## 2.7. Immunofluorescence

Cells were plated on coverslips, cultured in a six-well plate and then subjected to appropriate treatment. Cells were fixed with acetone:methanol (1:1), blocked with 5% normal goat serum for 30 min at 37 °C, and then incubated with anti-p65 or anti-p50 or PBS overnight at 4 °C, followed by incubation with Cy3-conjugated anti-rabbit IgG (Sigma) for 30 min at 37 °C. Finally, the coverslips were examined with a confocal laser scanning microscope (Olympus, Tokyo, Japan).

## 2.8. RT-PCR

1 µg of total RNA isolated by TRIzol reagent was subjected to cDNA synthesis by Superscript III reverse transcriptase (Invitrogen). The PCR reaction was then performed using 1 µl cDNA and a pair of primers specific for each gene. For the semi-quantitative PCR, the PCR products were visualized on a 1.5% agarose gel with EB staining. For real-time PCR, SYBR green real-time PCR master mix (Toyobo, Osaka, Japan) was employed. After denaturizing at 95 °C for 60 s, a two-step reaction was used in our reaction as the following, step 1: 95 °C 10 s; step 2: 95 °C 5 s, 60 °C 50 s, 40 cycles for step 2. Data were collected by Rotor-Gene 6000 (Corbett life science, Australia).

## 2.9. Two-tag system and immunoprecipitation

Wild-type CD146 cDNA and different mutants were cloned into both pcDNA3.1/myc-his(-)b and p3xFLAG-cmv-14. A pair of wild-type or mutated CD146 proteins fused with myc-tag or FLAG-tag at C-terminus were co-expressed in cells by co-transfecting corresponding plasmids into HUVEC cells. The interaction between myc- and FLAG-tagged CD146 wild-type or mutated proteins were then determined by immunoprecipitation with anti-FLAG mAb and followed immunoblot with anti-myc mAb. Briefly, cells co-transfected with two kinds of expression plasmids were harvested and lysed with RIPA Buffer [50 mM Tris–HCl pH 7.4, 1% NP-40, 0.25% Nadeoxycholate, 150 mM NaCl, 1 mM EDTA, 1 mM Na<sub>3</sub>VO<sub>4</sub>, 1 mM NaF, 1 mM PMSF and proteinase inhibitors]. Soluble fractions were pre-cleared with protein A-agarose and then incubated with anti-FLAG or normal IgG overnight at 4 °C. The immunocomplexes were captured by protein A-agarose and then subjected to Western blot using anti-Myc mAb.

Dimerization Efficiency was calculated from Western blot results. Firstly, the band density of anti-Myc in whole cell lysates (WCL) were measured and normalized by the band density of anti-FLAG in WCL. The value was then designated as anti-Myc-WCL. Secondly, band density of anti-Myc in anti-FLAG precipitates

was measured and the value was designated as anti-Myc-IP. Dimerization efficiency was obtained by the following formula: [dimerization efficiency = anti-Myc-IP/anti-Myc-WCL] and relative values were calculated by setting the value from the control sample as 1.

## 3. Results

### 3.1. CD146 was required for SMMC 7721-CM-stimulated tubular morphogenesis

To study tumor-induced angiogenesis, conditional medium from hepatocarcinoma cells SMMC 7721, designated as SMMC 7721-CM, was used to stimulate human endothelial cells. We utilized siRNA duplex specifically against CD146 to silence the expression of endogenous endothelial CD146 and directly tested the role of CD146 in tumor secretions-induced angiogenesis. Tube formation assay, the *in vitro* test for angiogenesis, was employed to examine the morphology and function of endothelial cells expressing different levels of CD146 under the treatment of SMMC 7721-CM. HUVECs with different transfections and treatments were placed on Matrigel for 6 h and results showed that SMMC 7721-CM accelerated and promoted the tube formation. However, cells with CD146 knockdown could not form capillary-like tube in response to SMMC 7721-CM and the total tube length was even lower than the basal level (Fig. 1A and B). Restoring CD146 levels by co-transfecting CD146 expression plasmids with siRNA-CD146 could rescue the tubular morphogenesis of HUVECs. Moreover, migration assays using collagen-coated transwell model also confirmed that the increased motility of endothelial cells in response to tumor secretions required CD146 (Fig. 1C). Therefore, our data indicated that endothelial CD146 played a crucial role in the pathological angiogenesis stimulated by tumor cell secretions.

### 3.2. CD146 contributed to the activation of p38/IKK/NFκB signaling cascade

Since blockage of NFκB expression was showed to efficiently impair angiogenesis (Miyake et al., 2006); and therapeutic anti-CD146 mAb, namely AA98, might suppress NFκB activation (Bu et al., 2006), we then checked whether endothelial CD146 promoted or mediated tumor angiogenesis by contributing to the activation of NFκB signal pathway. HUVEC cells transfected with siRNA duplex targeting either CD146 or GFP, were treated with SMMC 7721-CM. Then the whole cell lysates (WCLs), as well as the nuclear extracts (NEs) and cytoplasmic fractions (CPs), were prepared and subjected to Western blot analysis using a panel of antibodies against NFκB signaling molecules. As shown in Fig. 2A, the increase of NFκB p65 and p50 in nucleus, the decrease of IκBα in cytoplasm and the phosphorylation of both IKK and IκBα, stimulated by SMMC 7721-CM, were remarkably blocked by siRNA-CD146. Conversely, NFκB signaling pathway was re-activated upon restoration of CD146 expression (Fig. 2Ai, lane 4). Some of these changes in protein amounts of signal mediators were quantified by measuring the band density (Fig. 2Aii). Since MAPK pathway was found to be upstream of IKK in activating NFκB in endothelial cells (Ulfhammer et al., 2006), we next measured phosphorylation of p38, as an indication of p38 activation, in Western blot assay. Results showed that p38 was activated under the stimulation of SMMC 7721-CM in HUVECs, but this increased activity was abrogated by silencing CD146 and restored by further resuming CD146 expression (Fig. 2B). Nevertheless, the activity of another MAPK, ERK1/2, had been found unchanged regardless of CD146 expression levels (data not shown).



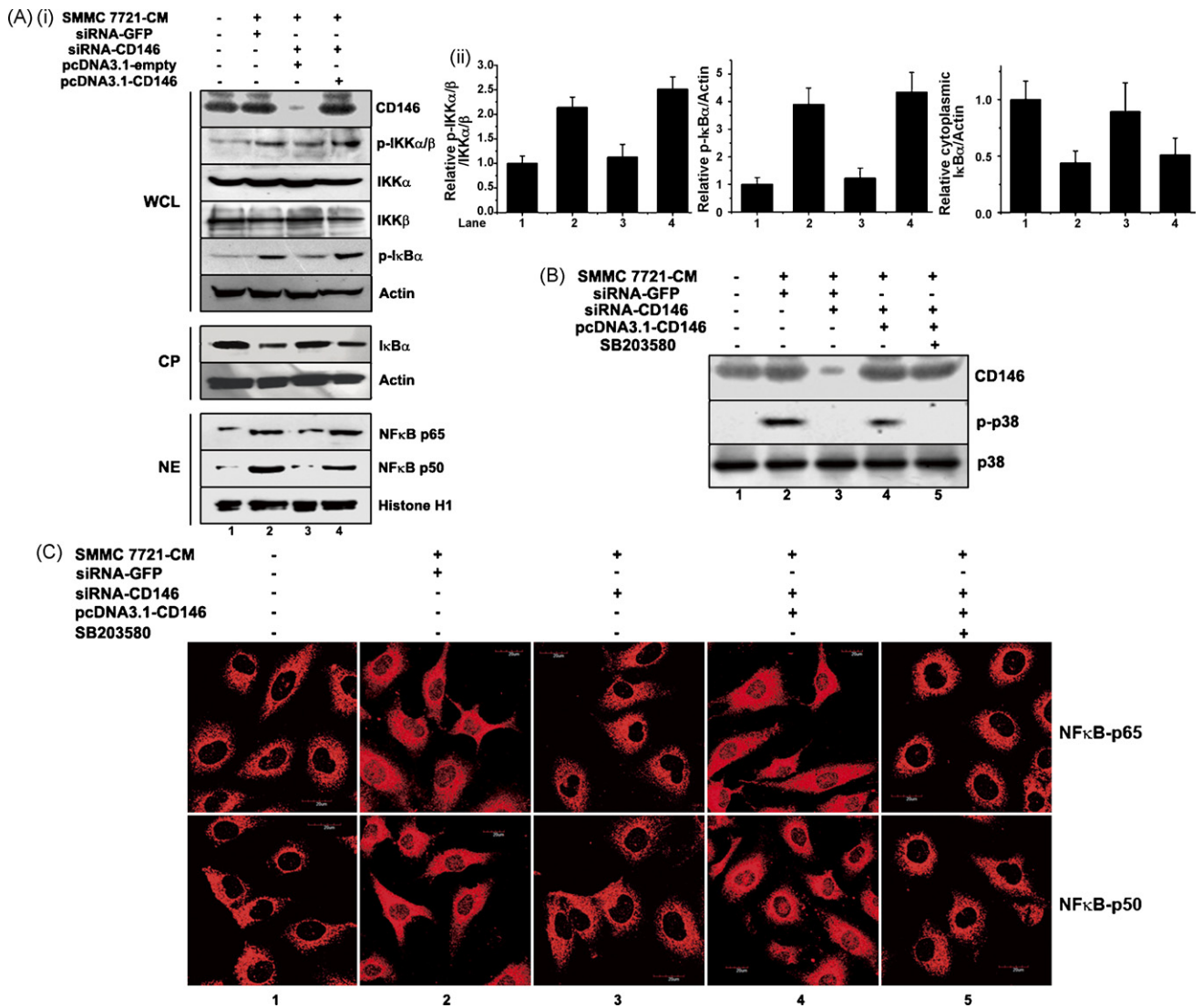


**Fig. 2.** CD146 contributed to p38/IKK/NFκB signaling cascade activation in response to SMMC 7721-CM. The whole cell lysates (WCL), cytoplasmic fraction (CP) and nuclear extracts from HUVEC cells under indicated treatments were subjected to Western blot analyses using indicated specific antibodies (Ai). The results of Western blot were quantified by measuring the band density and then normalized with internal controls, such as IKKα/β and Actin. By setting the untreated samples (lane 1) as 1, results of experimental samples (lanes 2–4) were presented in bar graphs as the mean ± S.D. of relative values from three independent assays (Aii). Cells, co-transfected with siRNA-CD146 and pcDNA3.1-CD146, were treated with SMMC 7721-CM alone or both of CM and p38 MAPK inhibitor, SB203580 (10 mM). Cells were then lysed for Western blot assays (B) or immunostaining with specific anti-p65 and anti-p50 antibodies (C).

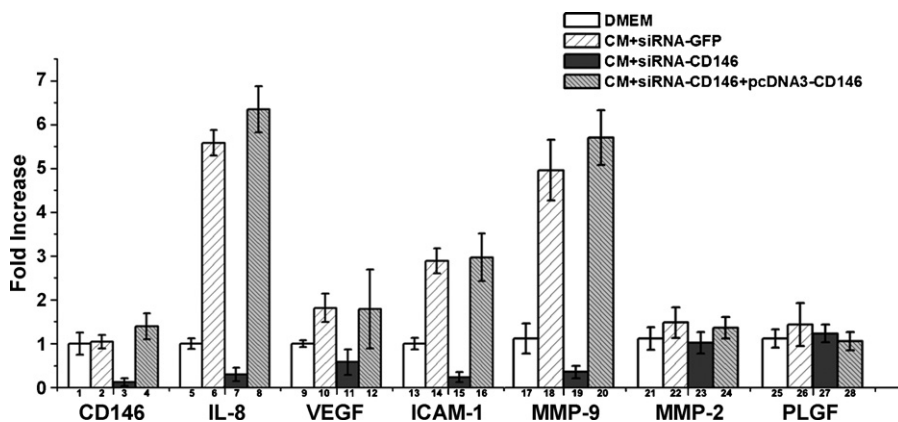


**Fig. 3.** Some NFκB-driven pro-angiogenic factors were up-regulated by tumor secretions in a CD146-dependent manner. HUVEC cells under indicated treatments were subjected to real-time PCR analyses for determining the transcripts levels of CD146, IL-8, VEGF, ICAM-1, MMP-9, MMP-2 and PLGF, using specific primers. The bar graph represented at least three independent tests and the transcription levels were presented as relative fold increase.

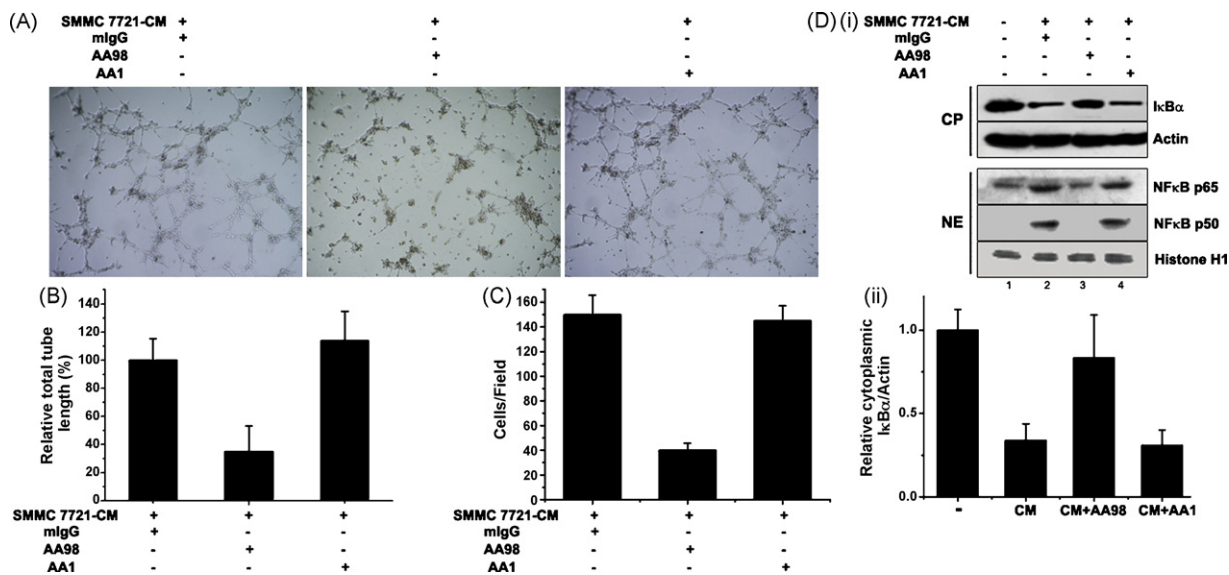


**Fig. 4.** AA98 not AA1 inhibited SMMC 7721-CM-induced tube formation and NFκB activation. HUVEC cells, stimulated with SMMC 7721-CM, were treated with 50 μg/ml of mlgG or AA98 or AA1. These cells were used in both tube formation assay (A), of which results were presented as relative total tube lengths (B), and cell migration assay (C). Then the nuclear extracts and cytoplasmic fractions were prepared for Western blotting analysis (Di) and results were quantified (Dii).

2. For studying the inducibility of dimerization, HUVECs were co-transfected with pcDNA3.1-Myc-CD146 and pCMV-3XFLAG-CD146 and then treated with SMMC 7721-CM and mAb AA98 or AA1. Co-IP and Western blot assay were performed. Results showed that secretions from SMMC 7721 markedly enhanced the dimerization of CD146 and this increased interaction was abrogated by only AA98 but not AA1 (Fig. 5A and B). Therefore, the evidence that AA98, not AA1, could disturb CD146 dimerization indicated that being different from AA1's epitope, AA98's epitope, which was structurally or topologically sheltered upon AA98 binding, might contain some amino acids essential for the dimerization of CD146 protein.

Together, completely different effects of these two anti-CD146 mAbs in both CD146-mediated signaling and dimerization suggested the different positions, roles and even importance of the two epitopes recognized by AA98 and AA1 respectively. Further identi-

fying them may lead us to discover the functional domain or site on CD146 protein.

### 3.6. Identification of fine epitopes of anti-CD146 mAbs, AA98 and AA1

The extracellular region of CD146 consists of five Ig-like domains, V-V-C2-C2-C2, corresponding to D1-D5, and each of them contains a theoretical disulfide bond. Based on our previous data, we designed and constructed a serial of recombinant fractions and full-length cDNA mutants of CD146, as illustrated in Fig. 6A. It was found that AA98 could only bind the fraction D4-5, the fused two IgC2 domains proximal to cell membrane, in non-reducing condition (Fig. 6B, upper and middle panels), implying that the epitope of AA98 was possibly disulfide bond-based. Therefore, we constructed

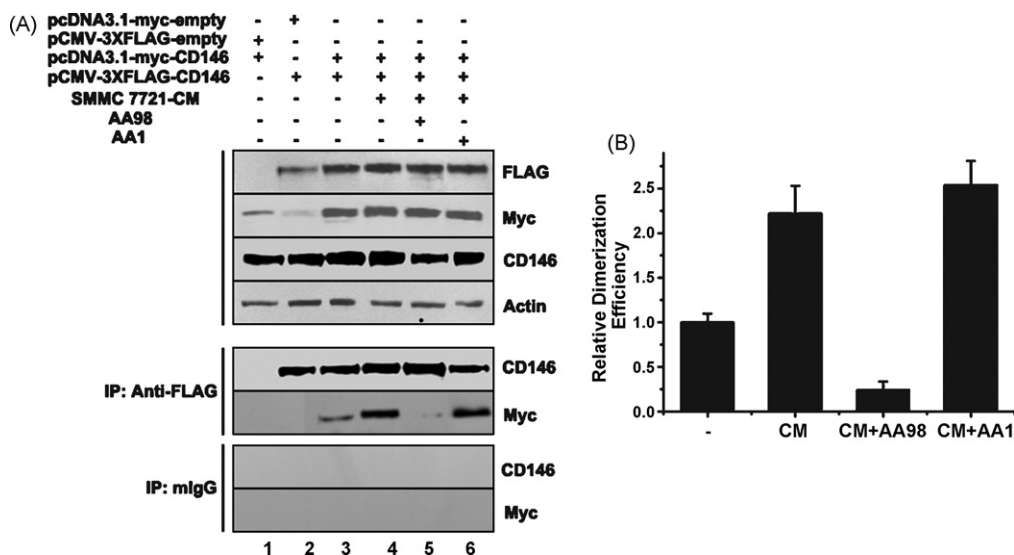


**Fig. 5.** AA98 but not AA1 inhibited CD146 dimerization. Myc-tagged CD146-expressing pcDNA3.1 vectors and FLAG-tagged CD146-expressing pCMV plasmids were co-transfected into HUVECs. Then cells were treated with SMMC 7721-CM or not in the presence of AA98 (50 μg/ml) or AA1 (50 μg/ml). Whole cell lysates were immunoprecipitated with anti-FLAG or mlgG and the immunoprecipitates were analyzed by Western blotting (A). Cell lysates without IP (WCL) were also subjected to Western blot assays to monitor the transfection efficiency. By measuring the band density, the Dimerization Efficiencies were calculated and relative values were determined by setting the value from control sample (lane1) as 1. The bar graph represented the mean ± S.D. of relative dimerization efficiency from three independent tests (B).

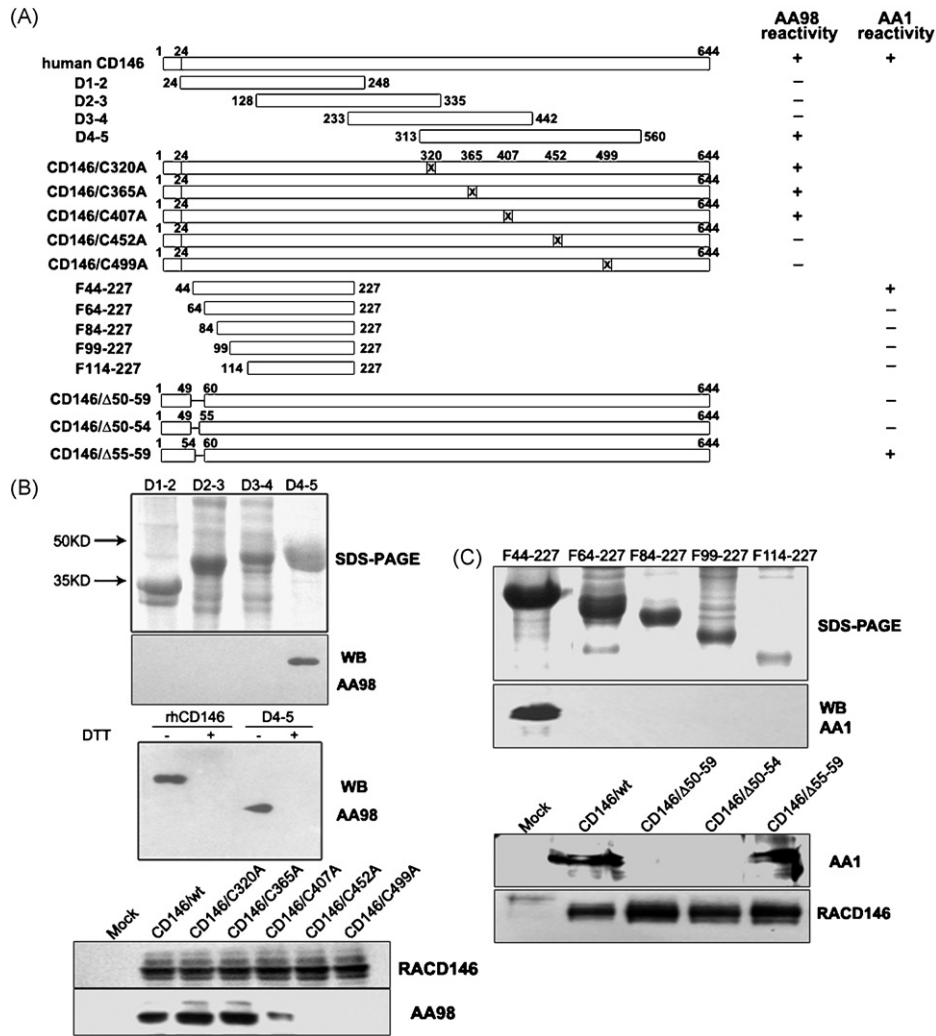


**Fig. 6.** Epitope mapping of anti-CD146 mAbs, AA98 and AA1. Schematic maps of different fractions of CD146 extracellular part and full-length CD146 mutants were illustrated (A). Recombinant fusions of CD146 domains were analyzed by SDS-PAGE and Western blot with AA98 in both reducing and non-reducing conditions. rhCD146 (aa24–552) served as positive control and 100 mM DL-Dithiothreitol, DTT, was added to create reducing condition (B, upper and middle panels). Expression vectors, encoding cysteine-mutated full-length CD146 proteins, were transfected into CHO cells. Whole cell lysates were subjected to immunoblot assays with AA98. Polyclonal antibody RACD146 was used to monitor the transfection efficiency and CD146/wt served as positive control (B, lower panels). Fractions based on CD146 D1–2 were expressed in *E. coli* and analyzed by SDS-PAGE and Western blot (C, upper panels). Full-length deletion mutants of CD146 were expressed in CHO cells and the whole cell extracts were taken to Western blot assays (C, lower panels).

five full-length CD146 mutants, carrying changes at the five cysteines respectively, in pcDNA3.1 vector and transfected them into human CD146-negative CHO cells. Results of Western blot using cell extracts showed that only mutating C452 and C499 could make the binding signal disappear (Fig. 6B, lowest panels). Rabbit anti-CD146 polyclonal antibodies, RACD146, were employed as positive control. These data indicated that C452 and C499, which should form a disulfide bond in D5, were essential for the binding of AA98 to CD146 protein. Importantly, disulfide bonds of C365–C407 and C452–C499 within CD146 protein were not only theoretically predicted but also practically observed when the recombinant CD146 D4–5 protein fraction was subjected to trypsin digestion and proteomic analysis under non-reducing conditions (Suppl. Fig. S1 and Table S1).

In order to get a fine epitope of AA1, we expressed recombinant fractions to test which amino acids were essential for AA1's recognition. As shown in the upper panels of Fig. 6C, only F44–227 but not F64–227 and other fractions could be detected by AA1, suggesting aa44–63 was the region bound by AA1. Further, deleting aa50–54 in full-length CD146 was sufficient for completely impairing the

binding of AA1 (Fig. 6D, lower panel), while RACD146 worked as a positive control. Thus, five amino acids in CD146 protein at the position of aa50–54 were indispensable for its association with AA1.

To sum up, works identified epitopes of two anti-CD146 mAbs, AA98 and AA1, one is functional for anti-angiogenesis but the other is not, were a conformational epitope depending on C452–C499 disulfide bond and a linear epitope containing aa50–54 respectively. Full-length CD146 mutant with mutation at C452 or C499 could not be recognized by AA98 and mutant lacking aa50–54 lost the binding of AA1. These mutants, found to be normally localized at the cell membrane, were used in the following studies.

### 3.7. C452 and C499 are essential for CD146-mediated tube formation and its dimerization

After proving the different binding sites of AA98 and AA1 on CD146, we tested the different roles of AA98 and AA1's epitopes in CD146-mediated signaling and tubular formation, as well as its dimerization. By co-transfecting HUVECs with siRNA-CD146 and various full-length CD146 mutants, we re-established differ-

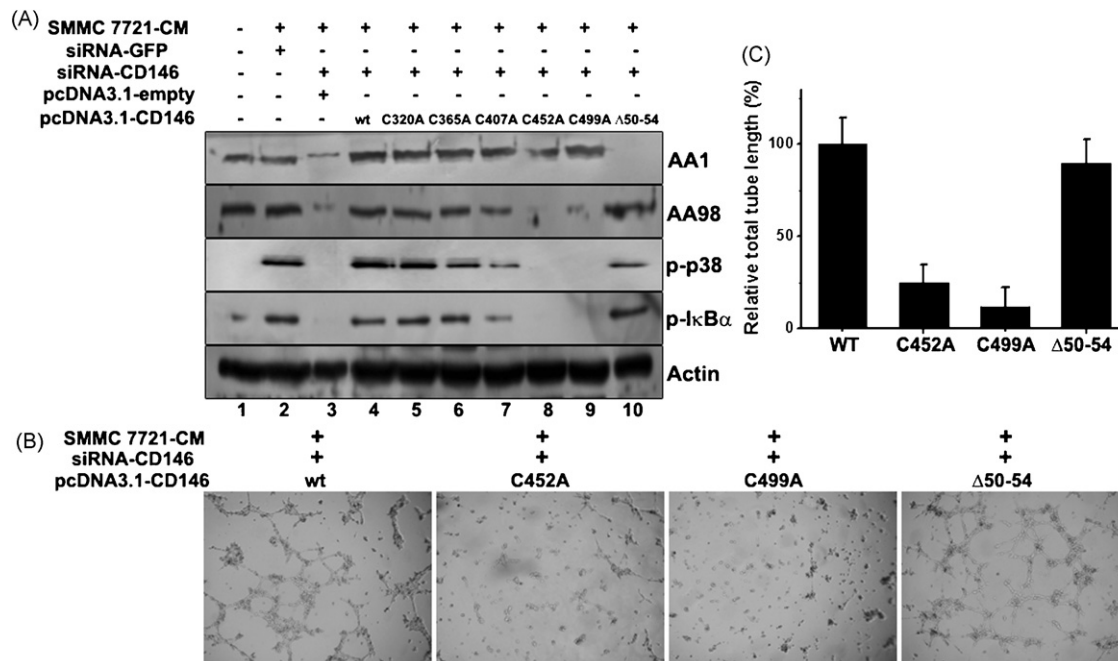


**Fig. 7.** C452 and C499 were indispensable for CD146-mediated tube formation and signaling. Wild-type or mutated CD146-expressing pcDNA3.1 vectors were respectively co-transfected with siRNA-CD146 into HUVEC cells which were then treated with SMMC 7721-CM. Cells were employed in Western blot using whole cells extracts (A) and tube formation assay (B and C).

ent mutants of CD146 in the cells and checked its status with AA1 and AA98 bindings in Western blot assays (Fig. 7A). The levels of phosphorylated p38 and I $\kappa$ B $\alpha$  were used to monitor the activation of CD146-mediated signaling cascades. Results showed that both p38 and I $\kappa$ B $\alpha$  could no longer be phosphorylated by SMMC 7721-CM treatment when HUVECs expressed CD146/C452A and CD146/C499A (Fig. 7A, lanes 8 and 9), whereas there were no difference between cells expressing CD146/wt and CD146/ $\Delta$ 50-54 (Fig. 7A, lanes 4 and 9). Also, mutating other cysteines, such as C320, C365 and C407, remained the function of CD146 unchanged in mediating p38 activation and I $\kappa$ B $\alpha$  phosphorylation. Furthermore, HUVECs expressing CD146/C452A and CD146/C499A could not undergo tubular morphogenesis as wild-type and other mutants did (Fig. 7B and C). Therefore, C452-C499 disulfide bond within the third IgC2 domain, proximal to cell membrane, were critical for CD146-mediated *in vitro* angiogenesis upon tumor secretion stimulation.

Dimerization of these CD146 mutants were tested by the two-tag system mentioned previously. We constructed the plasmids expressing FLAG-tagged or Myc-tagged CD146 mutants, transfected them into HUVECs, and measured the dimerization levels. As shown in Fig. 8, when two kinds of vectors, pcDNA3.1-Myc and pCMV-3XFLAG, were co-transfected into the same cells, CD146/C452A and CD146/C499A could not detectably form a dimer and be detected by anti-Myc in anti-FLAG immunoprecipitates (Fig. 8A, lanes 9–12). Nevertheless, other mutants, including changes at other three cysteines and deletion of AA1's epitope, still had the capability of maintaining dimerization in quiescence and up-regulating dimerization in response to tumor secretions as the wild-type CD146 did (Fig. 8B, lanes 1–8 and 13–14). These data implied that C452 and C499 were indispensable for protein-protein interaction during the process of CD146 dimerization. Moreover, dimerization between CD146/wt and CD146/C452A or CD146/C499A was severely compromised and the association between CD146/C452A and CD146/C499A cannot be detected (Fig. 8C and D). It further confirmed the involvement of the C452A–C499A disulfide bond in the dimerization process.

#### 4. Discussion

Although CD146 has been implicated to be up-regulated in blood capillaries, hematogenous sprouts and tumor vessels (Sers et al., 1994), the exact role of CD146 in angiogenesis, especially tumor angiogenesis, is still unclear. In the present study, we stimulated human endothelial cells with conditional medium from human liver cancer cells and observed that the promotion of *in vitro* tubular morphogenesis of HUVECs required endogenous endothelial CD146 expression. Further analysis discovered that CD146 was indispensable for the activation of p38/IKK/NF $\kappa$ B signaling cascade and subsequent up-regulation of pro-angiogenic genes, including at least IL-8, VEGF, ICAM-1 and MMP-9, in response to tumor secretions. Therefore, we for the first time uncovered the promotive role of CD146 in tumor-induced angiogenesis by proving CD146 was required for activating pro-angiogenic p38/IKK/NF $\kappa$ B signaling and increasing endothelial motility.

Since the potential ligand of CD146 has still not been identified, it is mysterious why CD146 is so essential for the activation of NF $\kappa$ B in endothelium during tumor-induced angiogenesis. NF $\kappa$ B signaling, as an important drive in pathological endothelial activation, is mainly induced by pro-inflammatory factors. However, in our study it was shown that CD146 knockdown influenced neither TNF- $\alpha$  nor IL1- $\beta$ -induced NF $\kappa$ B activation, which indicated that CD146 was probably not involved in TNFR- and IL1Rs-initiated NF $\kappa$ B signaling (Fig. S2A). Moreover, SMMC 7721 expressed no TNF- $\alpha$  and a very low level of IL-1 $\beta$  (Fig. S2B), but neutralizing IL-1 $\beta$  with antibodies could not discernibly impair SMMC 7721-CM-induced NF $\kappa$ B activation, indicating IL-1 $\beta$  was not the major trigger for the signaling (Fig. S2C, lane 3). Moreover, specific PI3K inhibitor was also unable to repress the NF $\kappa$ B activation requiring CD146 (Fig. S2C, lane 4), suggesting that CD146 was not engaged in the possible crosstalk between growth factors-induced PI3K/Akt pathway and NF $\kappa$ B signaling. As CD146 cannot fit in these known NF $\kappa$ B-activating pathways, it is possible that by the binding of the unknown ligand, present in the tumor secretions, CD146 directly mediated the outside-in signaling, which in turn activate



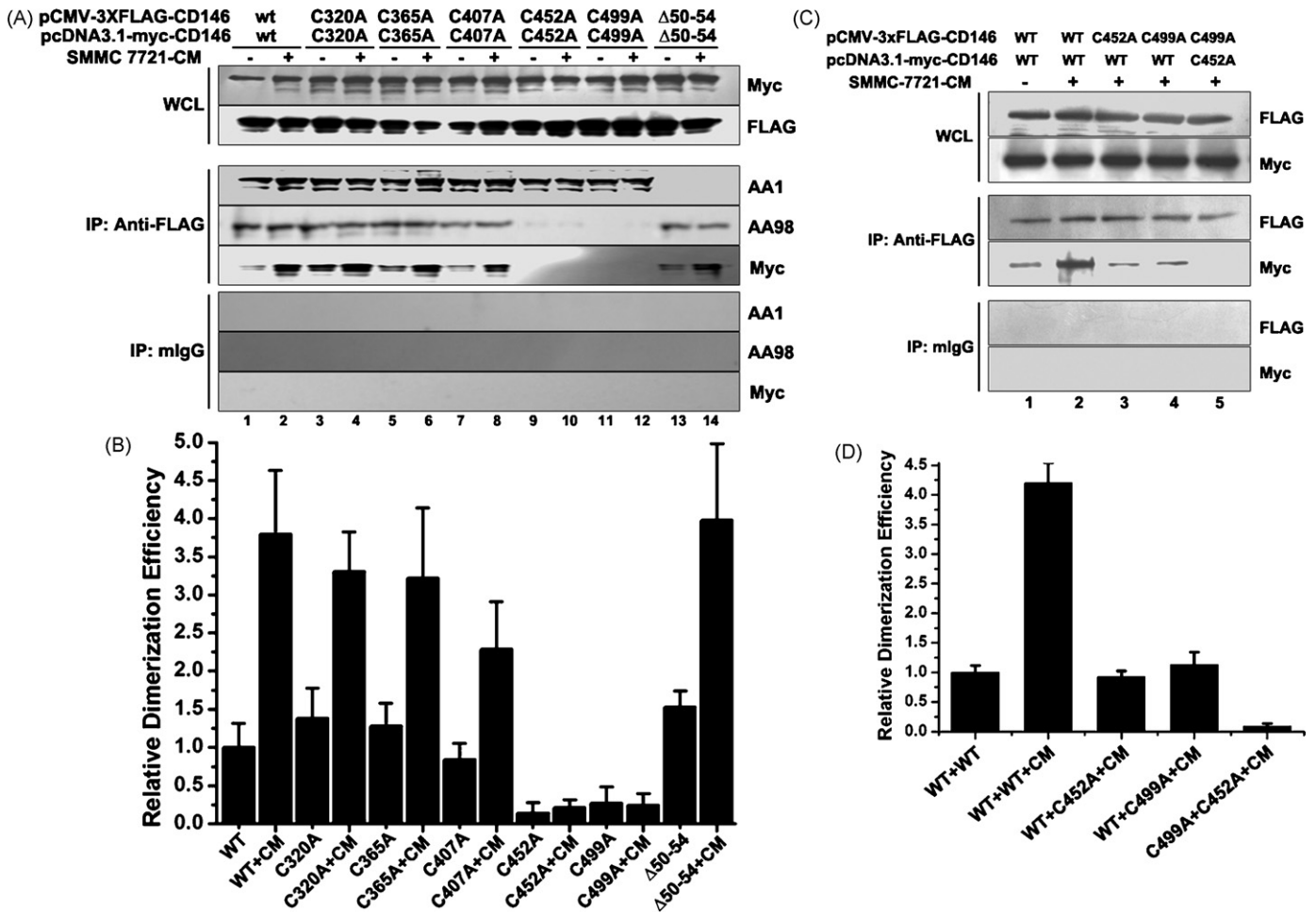


**Fig. 8.** C452–C499 disulfide bond was essential for CD146 dimerization. Indicated two kinds of vectors, pcDNA3.1-Myc and pCMV-3XFLAG, containing wild-type or mutated CD146 cDNAs, were co-transfected into HUVEC cells and then treated with SMMC 7721-CM or not. Immunoprecipitation and followed Western blotting assays were carried out (A and C); and the dimerization efficiency were calculated and set as relative values. The bar graph represented the mean  $\pm$  S.D. of relative dimerization efficiency from the results of three independent IP-WB tests (B and D).

p38/IKK/NF $\kappa$ B cascade. Thus, a careful analysis of the conditional medium composition might help identify this potential ligand.

Interestingly, a close correlation between signaling mediation and dimerization of CD146 was found in present studies. Secretions from SMMC 7721 induced both CD146-dependent NF $\kappa$ B signaling and its dimerization, leading to enhanced *in vitro* angiogenesis; and these up-regulations were coincidentally abrogated by either adding anti-CD146 mAb AA98 or disrupting the C452–C499 disulfide bond. It suggested that CD146 might serve as a membrane signal receptor, of which the dimerization or oligmerization triggers the signal transduction upon ligand binding. Given these observations, we hypothesized that the potential ligand binding site of CD146 was structurally based on C452–C499 disulfide bond and it was sheltered by the binding of AA98. Moreover, this disulfide bond could also be the structural basis of how CD146 formed a dimer and how it initiated downstream signaling.

In recent years, owing to the specific abilities to target tumors, therapeutic monoclonal antibodies have become more and more effective and rather promising in clinical cancer treatment. However, among thousands of monoclonal antibodies against tumor-associated antigens, the number of functional ones with tumor-suppressing activities is limited, which could be partially explained by the distinct epitopes recognized by anti-cancer mAbs. For example, anti-EGFR mAb Cetuximab was found to interact exclusively with domain III of sEGFR, partially occluding the ligand

binding region and sterically preventing the receptor from adopting the extended conformation required for dimerization (Li et al., 2005). That is consistent with our study that mAb AA98 perturbed CD146 dimerization and possibly covered up the potential ligand binding site. Moreover, Wang et al.'s study on anti-HER2 antibodies showed that non-inhibitory antibody HF only recognized N-terminal portion of erbB2 ectodomain, but inhibitory antibody Herceptin, also known as Trastuzumab, bound to C-terminal portion of it exclusively (Wang et al., 2004). Excitingly, it almost exactly matches our observations that non-functional AA1 bound the N-terminus (aa50–54) while inhibitory AA98 recognized a conformational epitope harbored in D4–5, very proximal to the membrane. Thus, the present study offers another instance to understand how the therapeutic monoclonal antibody against tumor-associated antigen works and hopefully could benefit drug development in the further.

#### Acknowledgements

We sincerely thank Mr. Peng Xue and Ms. Zhensheng Xie for their kind helps in the mass spectrometric analysis. This work is partly supported by the National High-tech R&D Program of China (863 Program) (2006AA02A245), the National Basic Research Program of China (973 Program) (2006CB910901, 2009CB521700), the National Natural Science Foundation of China (Nos. 90406020, 30672436)

and the Knowledge Innovation Program of the Chinese Academy of Sciences (KSCX2-YW-R-121).

## Appendix A. Supplementary data

Supplementary data associated with this article can be found, in the online version, at doi:10.1016/j.biocel.2009.03.014.

## References

- Anfosso F, Bardin N, Frances V, Vivier E, Camoin-Jau L, Sampol J, et al. Activation of human endothelial cells via S-endo-1 antigen (CD146) stimulates the tyrosine phosphorylation of focal adhesion kinase p125(FAK). *J Biol Chem* 1998;273:26852–6.
- Anfosso F, Bardin N, Vivier E, Sabatier F, Sampol J, Dignat-George F. Outside-in signaling pathway linked to CD146 engagement in human endothelial cells. *J Biol Chem* 2001;276:1564–9.
- Bardin N, George F, Mutin M, Brisson C, Horschowski N, Frances V, et al. S-Endo 1, a pan-endothelial monoclonal antibody recognizing a novel human endothelial antigen. *Tissue Antigens* 1996;48:531–9.
- Barnes PJ, Karin M. Nuclear factor-kappaB: a pivotal transcription factor in chronic inflammatory diseases. *N Engl J Med* 1997;336:1066–71.
- Blackwell TS, Christman JW. The role of nuclear factor-kappa B in cytokine gene regulation. *Am J Respir Cell Mol Biol* 1997;17:3–9.
- Bowie A, Moynagh PN, O'Neill LA. Mechanism of NF kappa B activation by interleukin-1 and tumour necrosis factor in endothelial cells. *Biochem Soc Trans* 1996;24:25.
- Bu P, Gao L, Zhuang J, Feng J, Yang D, Yan X. Anti-CD146 monoclonal antibody AA98 inhibits angiogenesis via suppression of nuclear factor-kappaB activation. *Mol Cancer Ther* 2006;5:2872–8.
- Bu P, Zhuang J, Feng J, Yang D, Shen X, Yan X. Visualization of CD146 dimerization and its regulation in living cells. *Biochim Biophys Acta* 2007;1773:513–20.
- Guezguez B, Vigneron P, Lamerant N, Kieda C, Jaffredo T, Dunon D. Dual role of melanoma cell adhesion molecule (MCAM)/CD146 in lymphocyte endothelium interaction: MCAM/CD146 promotes rolling via microvilli induction in lymphocyte and is an endothelial adhesion receptor. *J Immunol* 2007;179:6673–85.
- Jaffe EA, Nachman RL, Becker CG, Minick CR. Culture of human endothelial cells derived from umbilical veins. Identification by morphologic and immunologic criteria. *J Clin Invest* 1973;52:2745–56.
- Johnson JP, Rothbacher U, Sers C. The progression associated antigen MUC18: a unique member of the immunoglobulin supergene family. *Melanoma Res* 1993;3:337–40.
- Kang Y, Wang F, Feng J, Yang D, Yang X, Yan X. Knockdown of CD146 reduces the migration and proliferation of human endothelial cells. *Cell Res* 2006;16:313–8.
- Leibovich SJ, Polverini PJ, Shepard HM, Wiseman DM, Shively V, Nuseir N. Macrophage-induced angiogenesis is mediated by tumour necrosis factor-alpha. *Nature* 1987;329:630–2.
- Li S, Schmitz KR, Jeffrey PD, Wiltzius JJ, Kussie P, Ferguson KM. Structural basis for inhibition of the epidermal growth factor receptor by cetuximab. *Cancer Cell* 2005;7:301–11.
- Miyake T, Aoki M, Shiraya S, Tanemoto K, Ogihara T, Kaneda Y, et al. Inhibitory effects of NFkappaB decoy oligodeoxynucleotides on neointimal hyperplasia in a rabbit vein graft model. *J Mol Cell Cardiol* 2006;41:431–40.
- Monaco C, Paleolog E. Nuclear factor kappaB: a potential therapeutic target in atherosclerosis and thrombosis. *Cardiovasc Res* 2004;61:671–82.
- Murley JS, Kataoka Y, Hallahan DE, Roberts JC, Grdina DJ. Activation of NFkappaB and MnSOD gene expression by free radical scavengers in human microvascular endothelial cells. *Free Radic Biol Med* 2001;30:1426–39.
- Nagata D, Mogi M, Walsh K. AMP-activated protein kinase (AMPK) signaling in endothelial cells is essential for angiogenesis in response to hypoxic stress. *J Biol Chem* 2003;278:31000–6.
- Naidu BV, Farivar AS, Woolley SM, Byrne K, Mulligan MS. Chemokine response of pulmonary artery endothelial cells to hypoxia and reoxygenation. *J Surg Res* 2003;114:163–71.
- Roebuck KA. Oxidant stress regulation of IL-8 and ICAM-1 gene expression: differential activation and binding of the transcription factors AP-1 and NF-kappaB (review). *Int J Mol Med* 1999;4:223–30.
- Sers C, Riethmuller G, Johnson JP. MUC18, a melanoma-progression associated molecule, and its potential role in tumor vascularization and hematogenous spread. *Cancer Res* 1994;54:5689–94.
- Shono T, Ono M, Izumi H, Jimi S, Matsushima K, Okamoto T, et al. Involvement of the transcription factor NF-kappaB in tubular morphogenesis of human microvascular endothelial cells by oxidative stress. *Mol Cell Biol* 1996;16:4231–9.
- St-Pierre Y, Couillard J, Van Themsche C. Regulation of MMP-9 gene expression for the development of novel molecular targets against cancer and inflammatory diseases. *Expert Opin Ther Targets* 2004;8:473–89.
- Ulfhammer E, Larsson P, Karlsson L, Hrafnkelsdottir T, Bokarewa M, Tarkowski A, et al. TNF-alpha mediated suppression of tissue type plasminogen activator expression in vascular endothelial cells is NF-kappaB- and p38 MAPK-dependent. *J Thromb Haemost* 2006;4:1781–9.
- Voronov E, Shouval DS, Krelin Y, Cagnano E, Benharroch D, Iwakura Y, et al. IL-1 is required for tumor invasiveness and angiogenesis. *Proc Natl Acad Sci USA* 2003;100:2645–50.
- Wang JN, Feng JN, Yu M, Xu M, Shi M, Zhou T, et al. Structural analysis of the epitopes on erbB2 interacted with inhibitory or non-inhibitory monoclonal antibodies. *Mol Immunol* 2004;40:963–9.
- Xie S, Luca M, Huang S, Gutman M, Reich R, Johnson JP, et al. Expression of MCAM/MUC18 by human melanoma cells leads to increased tumor growth and metastasis. *Cancer Res* 1997;57:2295–303.
- Yan X, Lin Y, Yang D, Shen Y, Yuan M, Zhang Z, et al. A novel anti-CD146 monoclonal antibody, AA98, inhibits angiogenesis and tumor growth. *Blood* 2003;102:184–91.
- Zhang Y, Zheng C, Zhang J, Yang D, Feng J, Lu D, et al. Generation and characterization of a panel of monoclonal antibodies against distinct epitopes of human CD146. *Hybridoma (Larchmt)* 2008;27:345–52.
- Zhen J, Lu H, Wang XQ, Vaziri ND, Zhou XJ. Upregulation of endothelial and inducible nitric oxide synthase expression by reactive oxygen species. *Am J Hypertens* 2008;21:28–34.